



## Convergent recombination cessation between mating-type genes and centromeres in selfing anther-smut fungi

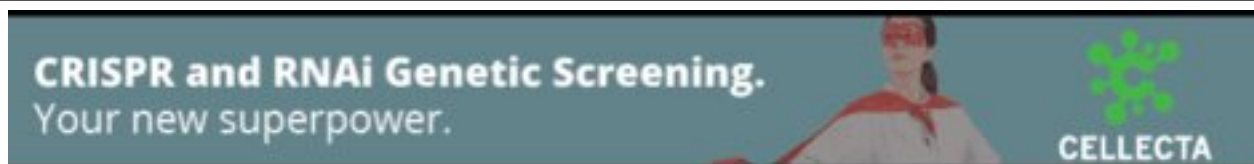
Fantin Carpentier, Ricardo C. Rodríguez de la Vega, Sara Branco, et al.

*Genome Res.* published online May 1, 2019

Access the most recent version at doi:[10.1101/gr.242578.118](https://doi.org/10.1101/gr.242578.118)

---

<b>P&lt;P</b>	Published online May 1, 2019 in advance of the print journal.
<b>Accepted Manuscript</b>	Peer-reviewed and accepted for publication but not copyedited or typeset; accepted manuscript is likely to differ from the final, published version.
<b>Creative Commons License</b>	This article is distributed exclusively by Cold Spring Harbor Laboratory Press for the first six months after the full-issue publication date (see <a href="http://genome.cshlp.org/site/misc/terms.xhtml">http://genome.cshlp.org/site/misc/terms.xhtml</a> ). After six months, it is available under a Creative Commons License (Attribution-NonCommercial 4.0 International), as described at <a href="http://creativecommons.org/licenses/by-nc/4.0/">http://creativecommons.org/licenses/by-nc/4.0/</a> .
<b>Email Alerting Service</b>	Receive free email alerts when new articles cite this article - sign up in the box at the top right corner of the article or <a href="#">click here</a> .



---

To subscribe to *Genome Research* go to:  
<https://genome.cshlp.org/subscriptions>

---

Published by Cold Spring Harbor Laboratory Press

1 **Convergent recombination cessation between mating-type genes and**  
2 **centromeres in selfing anther-smut fungi**

3 Fantin Carpentier\*†<sup>1</sup>, Ricardo C. Rodríguez de la Vega†<sup>1</sup>, Sara Branco<sup>1,2</sup>, Alodie Snirc<sup>1</sup>,  
4 Marco A. Coelho<sup>3,4</sup>, Michael E. Hood#<sup>5</sup>, Tatiana Giraud#<sup>1</sup>

5 † These authors contributed equally to the study

6 # These authors both supervised the study

7 <sup>1</sup> Ecologie Systématique Evolution, Bâtiment 360, Univ. Paris-Sud, AgroParisTech, CNRS, Université Paris-  
8 Saclay, 91400 Orsay, France

9 <sup>2</sup> Department of Microbiology and Immunology, Montana State University, Bozeman, MT 59717, USA (current  
10 address)

11 <sup>3</sup> UCIBIO-REQUIMTE, Departamento de Ciências da Vida, Faculdade de Ciências e Tecnologia, Universidade  
12 NOVA de Lisboa, 2829-516 Caparica, Portugal.

13 <sup>4</sup> Department of Molecular Genetics and Microbiology, Duke University Medical Center, Durham, NC 27710  
14 (current address)

15 <sup>5</sup> Department of Biology, Amherst College, Amherst, Massachusetts United State of America

16 \***Corresponding author:** Fantin Carpentier

17 Laboratoire Ecologie, Systématique et Evolution, Bâtiment 360, Université de Paris-Sud, 91405 Orsay  
18 cedex France

19 phone: +33 1 69 15 56 69 + 33 7 86 01 67 59 fax: +33 1 69 15 46 97

20 fantin.carpentier@gmail.com

21 **Running title:** Convergent recombination cessation in mating-type chromosomes

22 **Key words:** young sex chromosomes, selfing mating system, automixis, centromere, fungi,  
23 recombination suppression, bipolar, tetrapolar, convergence, breeding system transition,  
24 central fusion automixis, supergenes, *Microbotryum saponariae*, *Microbotryum lagerheimii*

## 25 **Abstract**

26 The degree of selfing has major impacts on adaptability and is often controlled by molecular  
27 mechanisms determining mating compatibility. Changes in compatibility systems are  
28 therefore important evolutionary events but their underlying genomic mechanisms are often  
29 poorly understood. Fungi display frequent shifts in compatibility systems and their small  
30 genomes facilitate elucidation of the mechanisms involved. In particular, linkage between the  
31 pre- and post-mating compatibility loci has evolved repeatedly, increasing the odds of gamete  
32 compatibility under selfing. Here, we studied the mating-type chromosomes of two anther-  
33 smut fungi with unlinked mating-type loci despite a selfing mating system. Segregation  
34 analyses and comparisons of high-quality genome assemblies revealed that these two species  
35 displayed linkage between mating-type loci and their respective centromeres. This  
36 arrangement renders the same improved odds of gamete compatibility as direct linkage of the  
37 two mating-type loci under the automictic mating (intra-tetrad selfing) of anther-smut fungi.  
38 Recombination cessation was found associated with a large inversion in only one of the four  
39 linkage events. The lack of trans-specific polymorphism at genes located in non-recombining  
40 regions and linkage date estimates indicated that the events of recombination cessation  
41 occurred independently in the two sister species. Our study shows that natural selection can  
42 repeatedly lead to similar genomic patterns and phenotypes, and that different evolutionary  
43 paths can lead to distinct yet equally beneficial responses to selection. Our study further  
44 highlights that automixis and gene linkage to centromeres have important genetic and  
45 evolutionary consequences, while being poorly recognized despite being present in a broad  
46 range of taxa.

47

## 48 **Introduction**

49 Mating systems reflect the degree of selfing/outcrossing in natural populations and impact  
50 gene flow, the accumulation of deleterious alleles and adaptability (Lande and Schemske  
51 1985; Igic et al. 2008; Charlesworth and Charlesworth 1987; Charlesworth et al. 1990;  
52 Charlesworth 2002; Hereford 2010; Lande 2015). Outcrossing can promote gene flow and  
53 therefore the rapid spread of beneficial alleles as well as the purge of deleterious alleles, while  
54 selfing is often associated with reproductive assurance and can help maintain favorable  
55 combinations of alleles at different loci. There is a wide diversity of mating systems in nature  
56 that strongly impact the evolution of organisms. Automixis with mating among products of a  
57 given meiosis that separated in the first meiosis division (“fusion of non-sister second division  
58 products” ; Lewis and John 1963), for example, is a little-known form of self-fertilization  
59 (Mogie 1986); such automixis is often called central fusion in animals, the term “fusion”  
60 referring to the union of gametes and the term “central” referring to the placement of the  
61 fusing gametes in an ordered tetrad (Suomalainen 1950; Goudie and Oldroyd 2014). This kind  
62 of automixis maintains heterozygosity at all loci for which there has been no recombination  
63 with the centromere (Engelstädter 2017; Zakharov 2005; Hood and Antonovics 2000;  
64 Lenormand et al. 2016; Hood and Antonovics 2004). This effect can extend over large  
65 portions of the genome when there is low levels of crossing-over (Hood and Antonovics 2000,  
66 2004). Automixis with central fusion can thus maintain long-term heterozygosity, which can  
67 lead to the sheltering deleterious alleles or may be beneficial in cases of advantageous  
68 overdominance (i.e., heterozygote advantage; Engelstädter 2017). Automixis and its genetic  
69 and evolutionary consequences are poorly studied despite being relatively frequent (Mogie  
70 1986), across a variety of taxa such as in fungi (Hood and Antonovics 2000; Zakharov 2005;  
71 Grognet et al. 2014; Menkis et al. 2008), plants (Asker 1980; Schön et al. 2009; Walker 1985;

72 Antonius and Nybom 1995; Cruden and Lloyd 1995), reptiles (Watts et al. 2006; Booth et al.  
73 2010; Booth and Schuett 2015), fishes (Chapman et al. 2007; Dudgeon et al. 2017; Feldheim  
74 et al. 2017), birds (Schut et al. 2008), crustaceans (Nougué et al. 2015), nematodes (Van der  
75 Beek et al. 1998) and insects (Normark 2003; Suomalainen et al. 1976; Oldroyd et al. 2008).

76 Evolutionary transitions between mating systems are known to be relatively frequent  
77 (Goldberg and Igić 2012; Goldberg et al. 2010; Nieuwenhuis et al. 2013; Chantha et al. 2013;  
78 Hanschen et al. 2018). Changes in the genetic determination of gamete production or  
79 compatibility often underlie transitions in mating systems, such as the evolution of a self-  
80 incompatibility system. For example, in many species mating can only occur between males  
81 and females, which enforces outcrossing, and sexes are often determined by sex chromosomes  
82 (Beukeboom and Perrin 2014). In angiosperms, mating can also be restricted by a self-  
83 incompatibility locus, which promotes outcrossing in hermaphroditic species by preventing  
84 mating between genotypes carrying identical alleles (Vekemans et al. 2014). In most fungi,  
85 gamete compatibility is controlled at the haploid stage and only cells carrying different alleles  
86 at the mating-type loci can successfully mate (Billiard et al. 2011, 2012).

87 Fungi provide excellent eukaryotic models for studying the genomic changes involved in  
88 gamete compatibility transition, as they display highly diverse and labile mate-recognition  
89 systems (Nieuwenhuis et al. 2013; Billiard et al. 2012, 2011), as well as relatively small and  
90 compact genomes that allow for high-quality genome assemblies (Badouin et al. 2015;  
91 Gladieux et al. 2014; Branco et al. 2017; Faino et al. 2015; Sonnenberg et al. 2016; Sun et al.  
92 2017a; Branco et al. 2018; Sun et al. 2017b). In basidiomycete fungi (e.g., rusts, smuts and  
93 mushrooms), mating type is most often controlled by two loci: (i) the PR locus, determining  
94 gamete fusion compatibility with a pheromone receptor and neighbouring pheromone genes,

95 and (ii) the HD locus, determining compatibility for post-mating development with two  
96 homeodomain genes (Coelho et al. 2017). To successfully mate and produce offspring, two  
97 gametes must carry different alleles at both loci. In most basidiomycetes, the PR and HD loci  
98 segregate independently (Raper 1966; Nieuwenhuis et al. 2013). Multiple independent events  
99 of linkage of the two mating-type loci have been documented in several fungal species  
100 (Branco et al. 2017; Bakkeren and Kronstad 1994; Nieuwenhuis et al. 2013; Sun et al. 2017b).  
101 Such control of gamete compatibility inherited as a single locus is advantageous under  
102 selfing as it increases the odds of gamete compatibility among the gametes of a given diploid  
103 individual (Fig. 1; Coelho et al. 2017).

104 The plant-castrating anther-smut fungi belonging to the highly-selfing basidiomycete genus  
105 *Microbotryum* are particularly good systems for studying the genomic changes underlying  
106 shifts in gamete compatibility systems. Before the radiation of this genus, recombination  
107 suppression extended around each of the PR and HD loci (Branco et al. 2017). Several  
108 *Microbotryum* species underwent independent transitions to complete linkage between the  
109 mating-type loci through various chromosomal rearrangements that brought the HD and PR  
110 loci onto the same chromosome (Branco et al. 2017, 2018). In some of these species, the  
111 cessation of recombination subsequently expanded far beyond the mating-type loci in several  
112 successive steps to include the majority of the mating type chromosomes (Branco et al. 2017,  
113 2018). Recombining pseudo-autosomal regions (PARs) remained at both edges of the mating-  
114 type chromosomes in many lineages (Branco et al. 2018).

115 The majority of studied anther-smut fungi undergo selfing by automixis (Hood and  
116 Antonovics 2000; Giraud et al. 2008; Vercken et al. 2010; Bueker et al. 2016; Gladieux et al.  
117 2011) and have linked mating-type loci (Branco et al. 2018). Here we studied two closely

118 related species, *Microbotryum lagerheimii* and *M. saponariae*, that have retained unlinked PR  
119 and HD mating-type loci located on different chromosomes (Fig.1; Hood et al. 2015), despite  
120 selfing mating systems (Fortuna et al. 2016; Abbate et al. 2018; Fortuna et al. 2018).  
121 However, *M. saponariae* displays the PR and HD mating-type loci completely linked to  
122 centromere of their respective chromosomes, which induces central fusion automixis and  
123 ensures the same odds of compatibility under selfing by automixis as would linkage between  
124 the mating-type loci (Fig. 1; Hood et al. 2015). While the mating-type loci are also known to  
125 be located on different chromosomes in *M. lagerheimii* (Branco et al. 2017), it is unclear  
126 whether the HD and PR loci are linked to the centromeres. In case they are linked to  
127 centromeres and given that *M. lagerheimii* and *M. saponariae* are sister species in available  
128 phylogenies (Fig. 2), recombination cessation with the centromeres could potentially predate  
129 their speciation event. An alternative hypothesis would be independent linkage events, with  
130 convergence for complete centromere linkage occurring in the two species after their  
131 divergence. In this study, we used segregation analyses and high-quality genome assemblies  
132 to investigate: 1) whether HD and PR loci are linked to the centromeres in *M. lagerheimii*, 2)  
133 whether linkage predates speciation between *M. lagerheimii* and *M. saponariae* or constitutes  
134 independent events, and 3) whether the PR and HD loci became linked to centromeres at  
135 similar dates in each species.

136

## 137 **Results**

### 138 **Linkage of mating-type loci to centromeres in *M. saponariae* and *M. lagerheimii***

139 To test whether recombination was suppressed between the mating-type loci and their  
140 respective centromere in *M. lagerheimii*, we analysed PR and HD mating-type loci  
141 segregation within ordered linear tetrads using allele-specific PCR markers for each mating-

142 type locus. When there is complete centromere linkage, alleles at both mating types always  
143 segregate at the first meiotic division, leading to the ordered linear *Microbotryum* tetrad with  
144 cells derived from opposite poles of meiosis I carrying alternate alleles at both the PR and HD  
145 loci (Fig. 1; Hood et al. 2015; Hood and Antonovics 2000). Conversely, when there is no  
146 centromere linkage of the mating type loci, mating-type alleles segregating at the second  
147 meiotic division results in only half the tetrads carrying alternate alleles at both loci in the  
148 opposite cells of the ordered linear tetrad (Figure 1). We found evidence supporting  
149 centromere linkage of mating-type loci in *M. lagerheimii*, with isolated meiotic products  
150 derived from opposite poles of meiosis I showing alternate alleles at both the PR and HD loci  
151 in all of the 78 meioses analysed. Given the number of tetrads analysed, the 95% confidence  
152 interval for the occurrence of recombination between at least one mating-type locus and its  
153 centromere was 0-5%. This indicates that the *M. lagerheimii* PR and HD loci are completely  
154 or nearly completely linked to their respective centromere, as in its sister species *M.*  
155 *saponariae* (Hood et al. 2015).

156 We compared the sequences of the mating-type chromosomes to investigate whether  
157 inversions could have contributed to linkage between mating-type loci and their centromeres.  
158 While the alternate HD mating-type chromosomes were collinear within both *M. saponariae*  
159 and *M. lagerheimii* (Figs. 3a and c), we observed a 51.4 kbp inversion between HD and the  
160 centromere in the *M. saponariae* lineage compared to the ancestral state, shared by *M.*  
161 *intermedium* and *M. lagerheimii* (Supplemental Figs. S2a and S3a). In both *M. saponariae*  
162 and *M. lagerheimii* the HD locus was located close to the centromere (distant by 138 kbp in  
163 *M. saponariae* and by 162 kbp in *M. lagerheimii*; Figs. 3a and 3c). In *M. lagerheimii* the  
164 alternate PR chromosomes ( $a_1$  and  $a_2$ ) also showed nearly complete collinearity (Fig. 3b), with  
165 only rearrangements around the PR locus, as typical in *Microbotryum* due to very old

166 recombination suppression in this region (Branco et al. 2017). In contrast, *M. saponariae*  
167 displayed a large pericentric inversion distinguishing the alternate PR chromosomes. This  
168 inversion involved 593 kbp in the  $a_1$  and 701 kbp in the  $a_2$  PR mating-type chromosomes,  
169 representing 50% and 52% of  $a_1$  and  $a_2$  PR chromosome lengths (Fig. 3d). The two edges of  
170 the inversion were very close the centromere and the PR locus (Fig. 3d; inversion boundaries  
171 were distant by 35 kbp from centromeres and by 0 kbp from the edge of the PR-proximate  
172 region with ancient recombination suppression). The inversion appeared derived in the  $a_2$  *M.*  
173 *saponariae* PR chromosome, as the *M. saponariae*  $a_1$  PR chromosome was highly collinear to  
174 the *M. lagerheimii*  $a_1$  and  $a_2$  PR chromosomes (Supplemental Fig. S1). No further  
175 rearrangements were present within the large inversion beyond those located in the PR-  
176 proximal region (Fig. 3d). A small additional inversion was observed towards the PAR in the  
177 short arm of the *M. saponariae*  $a_2$  PR mating-type chromosome (green region in Fig. 3d,  
178 involving 11 kbp and 20 kbp on the  $a_1$  and  $a_2$  PR mating-type chromosomes). This inversion  
179 may correspond to an additional step extending further recombination cessation towards the  
180 PAR.

181 Synonymous divergence ( $d_S$ ) between alleles associated to the alternative mating types at the  
182 genes located between the PR-proximal region and the centromere in *M. lagerheimii* and *M.*  
183 *saponariae* provided further evidence for complete centromere linkage of the PR mating-type  
184 loci. For all genes linked to a mating-type locus, the same allele remains associated with the  
185 same mating-type, so that alleles associated to the alternate mating types accumulate  
186 independent mutations, showing increasing divergence ( $d_S$ ) with time since the complete  
187 recombination cessation. To recover the history of recombination cessation, we plotted allelic  
188 divergence ( $d_S$ ) along the ancestral gene order, as subsequent rearrangements may blur  
189 historical steps (Branco et al. 2017). We used the mating-type chromosomes of an outgroup

190 species with independently segregating mating types (*M. intermedium*) as a proxy for the  
191 ancestral gene order; however, using the *M. lagerheimii* gene order gave similar conclusions  
192 given the few rearrangements observed (Supplemental Figs. S2 and S3; Branco et al. 2017).  
193 We observed very high levels of synonymous divergence around the PR and HD mating-type  
194 loci both in *M. lagerheimii* and *M. saponariae* (purple and blue genomic regions, respectively,  
195 Fig. 4). This result was expected given ancient recombination cessation proximal to each of  
196 the PR and HD mating-type loci (Branco et al. 2017). The non-zero  $d_S$  values between the  
197 PR-proximal region and the centromere in *M. saponariae* and *M. lagerheimii* supported  
198 complete linkage to the centromere. In highly selfing organisms such as anther-smut fungi,  
199 homozygosity is high at almost all genes (*i.e.*  $d_S=0$  between alleles on autosomes in a diploid  
200 individual; Supplemental Fig. S4) except in regions linked to mating-types (Branco et al.  
201 2018). The lower  $d_S$  values closer to the centromere than closer to the purple region, in both  
202 *M. saponariae* and *M. lagerheimii* (Figs. 4a and c), suggest stepwise extension of  
203 recombination cessation farther from the PR locus and to eventually reach the centromere.  
204 The synonymous divergence between the HD-proximal blue region and its centromere in both  
205 species was almost zero, although some genes exhibited non-zero  $d_S$  value (Figs. 4b and d).

206 We found increased transposable element content in the HD and PR chromosomes in *M.*  
207 *saponariae* and *M. lagerheimii* compared to their autosomes. There were differences within  
208 each species between  $a_1$  and  $a_2$  mating-type chromosomes (Supplemental Fig. S5). Such  
209 transposable element accumulation and differences between homologous chromosomes  
210 further supported complete recombination cessation.

211

212 **Absence of trans-specific polymorphism between centromeres and the HD- and PR-**  
213 **proximal regions in *M. saponariae* and *M. lagerheimii***

214 We used genealogies of genes located between centromeres and the HD- and PR-proximal  
215 blue and purple regions, respectively, to assess whether linkage of mating-type loci to  
216 centromeres in *M. saponariae* and *M. lagerheimii* derived from a single event predating their  
217 speciation or from independent events in each lineage. If recombination cessation predates  
218 speciation, the alleles associated to the alternative mating-types will cluster by mating type  
219 rather than by species (which is called trans-specific polymorphism), as the alleles will have  
220 been linked to mating types since before the speciation. In contrast, if linkage is more recent  
221 than speciation, alleles will cluster by species as recombination will have broken any allelic  
222 association with mating-type within species after speciation. None of the orthologous groups  
223 corresponding to genes located between the PR- or the HD-proximal purple and blue regions  
224 and their centromeres displayed trans-specific polymorphism shared by *M. saponariae* and *M.*  
225 *lagerheimii*. We could use nine genes in the HD mating-type chromosome (Supplemental Fig.  
226 S6a) and ten genes in the PR mating-type chromosomes (Supplemental Fig. S6b), for which  
227 both alleles were available in all species with available genomes (the genes are indicated by  
228 red arrows on Fig. 4). These findings indicate independent events of complete mating-type-  
229 loci-centromere linkage in *M. saponariae* and *M. lagerheimii*.

230 We found further support for recombination suppression occurring after *M. saponariae* and  
231 *M. lagerheimii* speciation by dating the differentiation between alleles associated with  $a_1$   
232 versus  $a_2$  mating types in gene genealogies. We computed a phylogenetic tree using the  
233 concatenated alignments of the nine and ten genes with both alleles available in all genomes  
234 and located between the HD-proximal region and the centromere, or the PR-proximal region  
235 and the centromere, respectively. We calibrated the tree nodes using the speciation date  
236 between *M. lychnidis-dioicae* and *M. silenes-dioicae*, previously estimated at 420 ky  
237 (Gladieux et al. 2011). Although these estimates are not robust absolute dates, they are useful

238 to obtain relative dates of speciation and chromosome evolution events. Recombination  
239 cessation between the PR-proximal purple region and the centromere was younger in *M.*  
240 *saponariae* and *M. lagerheimii* (95% confidence interval 171 – 302 and 80 – 158 ky,  
241 respectively, Fig.5a) than their speciation event (95% confidence interval 2,997 – 4,386 ky,  
242 Fig. 5b). The date of recombination cessation between the HD-proximal blue region and the  
243 centromere was even younger in both species (95% confidence interval 0.1 - 18 and 3 - 26 ky,  
244 respectively, Fig.5a).

245

## 246 **Discussion**

247 Here, we document convergent evolution of increased odds of gamete compatibility under  
248 automixis by independent linkage events of mating-type loci and centromeres in two closely  
249 related fungal species. Such linkage represents further convergence in gamete compatibility  
250 patterns with other congeneric lineages, that were previously shown to have achieved similar  
251 gamete compatibility odds through multiple independent direct linkage events between PR  
252 and HD mating-type loci (Branco et al. 2018). Linkage of the two mating-type loci, one to  
253 each other or to their centromere, are equally beneficial under automixis in terms of gamete  
254 compatibility odds (Fig. 1; Hood et al. 2015). We found here that the two mating-type loci in  
255 *M. lagerheimii*, while located on separate chromosomes, are completely linked to their  
256 respective centromeres, as in *M. saponariae*. Furthermore, we showed that in these sister  
257 species of anther-smut fungi such linkage occurred through independent recombination  
258 cessation events. Convergence of mating-type loci and centromere linkage seems to have also  
259 occurred at much larger phylogenetic scale within fungi. *Cryptococcus amyloletus*, a distant  
260 *Microbotryum* fungal relative, also displays both HD and PR genes linked to different  
261 centromeres (Sun et al. 2017a). Our study thus shows that natural selection can lead

262 repeatedly to similar genomic changes but also to distinct and equally beneficial solutions  
263 under a shared evolutionary pressure. These findings contribute to our understanding of  
264 evolution and the degree to which it is repeatable.

265 Segregation analyses showed that the HD and PR loci are linked to their respective  
266 centromere in *M. lagerheimii*, as previously shown in its sister species *M. saponariae* (Hood  
267 et al. 2015). While the inclusion of a finite number of analysed meiotic tetrads leaves the  
268 possibility that linkage to centromeres is only nearly complete, our genomic results support  
269 complete linkage in the PR chromosome. We found substantial differentiation between alleles  
270 associated to alternative mating-types at genes between the PR-proximal region and its  
271 centromere in both species, as well as a large inversion in *M. saponariae*. Additional evidence  
272 of complete recombination cessation is that the HD chromosome in *M. saponariae* and the PR  
273 chromosomes in both species are size dimorphic, with size co-segregating with mating type  
274 alleles (Hood et al. 2015). Chromosome size dimorphism is likely due to the differential  
275 transposable element amounts we found between alternate HD and PR chromosomes in each  
276 species.

277 The absence of trans-specific polymorphism and the more recent inferred linkage dates  
278 compared to the speciation event between *M. saponariae* and *M. lagerheimii* strongly support  
279 that recombination cessation was independent in the two species. The recent origins of  
280 complete linkage between the two mating-type loci and their centromeres in both species are  
281 corroborated by the low synonymous divergence values between  $a_1$  and  $a_2$ -associated alleles  
282 and the lack of extensive rearrangements in the regions without recombination between the  
283 mating-type locus proximal regions and the centromeres.

284 For linkage of mating-type loci to centromeres to be beneficial under selfing by automixis,  
285 both HD and PR mating-type genes need to be linked to their respective centromere  
286 (Zakharov 1986, 2005). However, for both *M. lagerheimii* and *M. saponariae*, the PR linkage  
287 to centromere evolved long before the HD-centromere linkage. The PR locus-centromere  
288 linkage alone provides no advantage concerning gamete compatibility odds when mating  
289 occurs within a tetrad; however the PR-centromere linkage may have been generated in  
290 several steps extending the recombination cessation region beyond mating-type genes, as  
291 previously described (Branco et al. 2017). This would be consistent with the apparent  
292 heterogeneity in the  $d_S$  values in the genes between the PR-proximal region and the  
293 centromere, with highest  $d_S$  values for genes closer to PR than to the centromere (Fig. 4).  
294 Under this hypothesis, expansion of the regions of suppressed recombination would have  
295 occurred through processes unrelated to the mating system, such as the accumulation and  
296 methylation of transposable elements in non-recombining regions and in their margins  
297 (Ponnikas et al. 2018). Once the PR-centromere linkage was achieved, selection for HD-  
298 centromere linkage may have occurred and been selected for increasing odds of compatibility  
299 under automixis.

300 Alternatively, the close physical proximity of the HD locus to the centromere may be  
301 sufficient to render recombination events infrequent enough that recombination cessation  
302 between the PR locus and its centromere would be immediately beneficial for increasing the  
303 odds of gamete compatibility under automixis. This hypothesis of rare recombination between  
304 the centromere and the HD would explain the very low  $d_S$  values in this region and the  
305 collinearity between  $b_1$  and  $b_2$  HD mating-type chromosomes in *M. saponariae* despite the  
306 inversion that occurred between HD and the centromere since its speciation from *M.*  
307 *lagerheimii*. This hypothesis is not incompatible with the PR-centromere linkage having

308 evolved by successive evolutionary steps. Low recombination rates have been invoked in sex  
309 chromosomes to explain low differentiation between alleles on X and Y chromosomes in  
310 some animals (Stöck et al. 2013).

311 Although inversions are often thought to play a major role in suppressing recombination  
312 (Wright et al. 2016; Lemaitre et al. 2009; Wang et al. 2012), non-recombining regions with  
313 conserved collinearity have been reported in several fungi (Grognet et al. 2014; Branco et al.  
314 2017; Jacobson 2005; Branco et al. 2018; Sun et al. 2017b). In this study, we only found  
315 inversions in the region with recent recombination cessation between the *M. saponariae* PR  
316 chromosomes. Finding that the limits of this inversion are precisely the centromere and the  
317 PR-proximal region is consistent with a role of inversions in recombination suppression,  
318 although we cannot exclude that the inversion occurred as a subsequent rearrangement after  
319 recombination cessation. The remaining mating-type loci and centromere linkage events  
320 occurred via different proximate mechanisms not involving rearrangements. Elucidating the  
321 proximal mechanisms suppressing recombination by exploring for example changes in DNA  
322 methylation and heterochromatin marks, as well as Spo11-dependent formation of double-  
323 strand breaks (Keeney 2008; Termolino et al. 2016), will be interesting in future studies.

324 Our results have general implications beyond mating systems in fungi and evolutionary  
325 convergence, providing an excellent illustration of the benefits of mating via central fusion  
326 automixis. Broader implication of central fusion automixis has been rarely considered, despite  
327 occurring in a wide range of taxa such as in fungi (Hood and Antonovics 2000; Zakharov  
328 2005; Grognet et al. 2014; Menkis et al. 2008), plants (Asker 1980; Schön et al. 2009; Walker  
329 1985; Antonius and Nybom 1995; Cruden and Lloyd 1995), and insects (Normark 2003;  
330 Suomalainen et al. 1976; Oldroyd et al. 2008). Theoretical models and reviews have

331 highlighted the evolutionary and genetic consequences of central fusion automixis in  
332 maintaining heterozygosity (Zakharov 1986; Hood et al. 2005; Zakharov 2005; Engelstädter  
333 2017; Antonovics and Abrams 2004), but few cases have been experimentally studied so far.  
334 Our findings illustrate how linkage to centromere under central fusion automixis can generate  
335 a sort of pseudo-linkage among genes on different chromosomes and preserve heterozygosity.  
336 Such maintenance of heterozygosity can be beneficial in a variety of cases (Ferreira and  
337 Amos 2006), such as the sheltering of deleterious alleles (Hood and Antonovics 2000) or  
338 overdominance in immune systems (Hraber et al. 2007) and other functions, as suggested at  
339 several loci in the case of the central fusion automictic Cape honeybees (Goudie et al. 2014).

340

## 341 **Materials and Methods**

342 To conduct segregation analyses we isolated *M. lagerheimii* haploid cells from opposite poles  
343 of meiosis I across replicate meioses from the same diploid parent using micromanipulation  
344 (Hood et al. 2015). We investigated mating-type segregation by PCR amplification of allele-  
345 specific markers. The *M. lagerheimii* strain used for segregation analyses was collected on  
346 *Lychnis flos-jovis* in Valle Pesio, Italy (GPS 44.188400, 7.670650).

347 Genome analyses were conducted in the *M. saponariae* and *M. lagerheimii* assemblies. We  
348 used alternative mating types isolated from a single diploid spore of *M. saponariae*  
349 parasitizing *S. officinalis* (cell 1268, PRAT 47, a<sub>1</sub> b<sub>1</sub>, and cell 1269, PRAT 48, a<sub>2</sub> b<sub>2</sub>) collected  
350 near Chiusa di Pesio, (GPS coordinates 44.31713297, 7.622967437 on July 8th, 2012). We  
351 used the *M. lagerheimii* genome previously published (a<sub>1</sub> b<sub>1</sub> and a<sub>2</sub> b<sub>2</sub> assemblies  
352 GCA\_900015505.1 and GCA\_900013405.1, respectively; (Branco et al. 2017). DNA was  
353 extracted with the QIAGEN Genomic-tip 100/G (ref. 10243; Courtaboeuf, France) and  
354 Genomic DNA Buffer Set (ref. 19060) following manufacturer instructions and using a

355 Carver hydraulic press (reference 3968, Wabash, IN, USA). Haploid genomes were  
356 sequenced using the P6/C4 Pacific Biosciences SMRT technology (UCSD IGM Genomics  
357 Facility La Jolla, CA, USA). Assemblies of the genomes were generated with the wgs-8.2  
358 version of the PBcR assembler (Koren et al. 2012). Contigs were aligned with optical maps of  
359 the two mating-type chromosomes obtained previously (Hood et al. 2015), with MapSolver  
360 software (OpGen), see statistics on assemblies in Supplemental Tables S1 and S2. We  
361 obtained orthologous groups with orthAgo (Ekseth et al. 2014) based on BLASTP+ 2.2.30  
362 followed by Markov clustering (Van Dongen 2000). We aligned the protein sequences of 780  
363 fully conserved single-copy genes with MAFFT v7.388 (Katoh and Standley 2013) and  
364 obtained the codon-based CDS alignments with TranslatorX (Abascal et al. 2010). We used  
365 RAxML 8.2.7 (Stamatakis 2006) to obtain maximum likelihood gene trees for all 780 fully  
366 conserved single-copy genes and a species tree with the concatenated alignment. We  
367 estimated synonymous divergence ( $d_s$ ) and its standard error with the yn00 program of the  
368 PAML package (Yang 2007).

369 We used nine orthologous groups (8,525 aligned codons) for dating the recombination  
370 cessation between the HD-proximal region and the centromere, and 10 orthologous (10,200  
371 aligned codons) groups for dating recombination cessation between the PR-proximal region  
372 and the centromere. Divergence times were estimated using BEAST v2.4.0 (Drummond and  
373 Rambaut 2007), with the XLM inputs being generated using BEAUTi (Drummond et al.  
374 2012).

375 Transposable elements were identified and annotated *de novo* in the high-quality genome  
376 assemblies, using both LTR-harvest (defaults parameters; Ellinghaus et al. 2008); and  
377 RepeatModeler (defaults parameters; Smit and Hubley 2015). We identified *de novo*

378 centromeric-specific repeats (Melters et al. 2013) using Tandem-Repeat Finder (TRF v.  
379 4.07b; Benson 1999), see Additional file 1.

380

### 381 **Data access**

382 The PacBio (Pacific Biosciences) genome assemblies from this study have been submitted to  
383 the European Nucleotide Archive (ENA; <https://www.ebi.ac.uk/ena>) under accession number  
384 GCA\_900015975 for the a<sub>1</sub> genome and GCA\_900015475 for the a<sub>2</sub> genome of *Microbotryum*  
385 *saponariae* from *Saponaria officinalis*.

386

### 387 **Acknowledgments**

388 This work was supported by the ERC starting grant GenomeFun 309403, the NSF DEB-  
389 1115765 and NIH R15GM119092 grants to MEH, the Marie Curie European grant 701646  
390 and the Montana State University Agricultural Research Station to SB, and postdoctoral  
391 fellowship (SFRH/BPD/79198/2011) from Fundação para a Ciência e a Tecnologia, Portugal  
392 to M.A.C. We thank Cécile Fairhead for help with DNA extraction. PacBio sequencing was  
393 conducted at the IGM Genomics Center, University of California, San Diego, La Jolla, CA.

394

### 395 **Author contributions**

396 TG and MEH designed and supervised the study. TG, MEH and SB contributed to obtain  
397 funding. MEH, AS and TG obtained the genomes. FC, RRDLV, SB and MAC performed the  
398 genomic analyses. MEH and AS performed the segregation analyses. FC, TG and MEH wrote  
399 the manuscript with contributions from all other authors.

400

401 **Disclosure declaration.** We declare no competing financial interests.

402

403

404

405

## 406 **References**

407 Abascal F, Zardoya R, Telford MJ. 2010. TranslatorX: Multiple alignment of nucleotide sequences

408 guided by amino acid translations. *Nucleic Acids Res* **38**(Web Server Issue): W7-13.

409 Abbate J, Gladieux P, Hood ME, De Vienne DM, Antonovics J, Snirc A, Giraud T. 2018. Co-occurrence

410 among three divergent plant-castrating fungi in the same *Silene* host species. *Mol Ecol* **27**(16):

411 3357–3370.

412 Antonius K, Nybom H. 1995. Discrimination between sexual recombination and apomixes/automixis

413 in a *Rubus plant* breeding programme. *Hereditas* **123**(3): 205–213.

414 Antonovics J, Abrams JY. 2004. Intratetrad mating and the evolution of linkage relationships.

415 *Evolution (N Y)* **58**(4): 702–709.

416 Asker S. 1980. Gametophytic apomixis: elements and genetic regulation. *Hereditas* **93**(2): 277–293.

417 Badouin H, Hood ME, Gouzy J, Aguilera G, Siguenza S, Perlin MH, Cuomo CA, Fairhead C, Branca A,

418 Giraud T. 2015. Chaos of rearrangements in the mating-type chromosomes of the anther-smut

419 fungus *Microbotryum lychnidis-dioicae*. *Genetics* **200**(4): 1275–1284.

420 Bakkeren G, Kronstad JW. 1994. Linkage of mating-type loci distinguishes bipolar from tetrapolar

421 mating in basidiomycetous smut fungi. *Proc Natl Acad Sci* **91**(15): 7085–7089.

422 Benson G. 1999. Tandem repeats finder: a program to analyze DNA sequences. *Nucleic Acids Res*

- 423           **27**(2): 573–580.
- 424   Beukeboom LW, Perrin N. 2014. *The evolution of sex determination*. Oxford University Press, USA.
- 425   Billiard S, López-Villavicencio M, Devier B, Hood ME, Fairhead C, Giraud T. 2011. Having sex, yes, but  
426       with whom? Inferences from fungi on the evolution of anisogamy and mating types. *Biol Rev*  
427       **86**(2): 421–442.
- 428   Billiard S, Lopez-Villavicencio M, Hood ME, Giraud T. 2012. Sex, outcrossing and mating types:  
429       unsolved questions in fungi and beyond. *J Evol Biol* **25**: 1020–1038.
- 430   Booth W, Johnson DH, Moore S, Schal C, Vargo EL. 2010. Evidence for viable, non-clonal but  
431       fatherless *Boa* constrictors. *Biol Lett* **7**(2): 253–256.
- 432   Booth W, Schuett GW. 2015. The emerging phylogenetic pattern of parthenogenesis in snakes. *Biol J*  
433       *Linn Soc* **118**(2): 176–186.
- 434   Branco S, Badouin H, Rodríguez de la Vega RC, Gouzy J, Carpentier F, Aguilera G, Siguenza S,  
435       Brandenburg J-T, Coelho MA, Hood ME, et al. 2017. Evolutionary strata on young mating-type  
436       chromosomes despite the lack of sexual antagonism. *Proc Natl Acad Sci* **114**(27): 7067–7072.
- 437   Branco S, Carpentier F, Rodríguez de la Vega RC, Badouin H, Snirc A, Le Prieur S, Coelho MA, de  
438       Vienne DM, Hartmann FE, Begerow D, et al. 2018. Multiple convergent supergene evolution  
439       events in mating-type chromosomes. *Nat Commun* **9**(1): 2000.
- 440   Bueker B, Eberlein C, Gladieux P, Schaefer A, Snirc A, Bennett DJ, Begerow D, Hood ME, Giraud T.  
441       2016. Distribution and population structure of the anther-smut *Microbotryum silenes-acaulis*  
442       parasitizing an arctic-alpine plant. *Mol Ecol* **25**(3): 811–824.
- 443   Chantha SC, Herman AC, Platts AE, Vekemans X, Schoen DJ. 2013. Secondary evolution of a self-  
444       incompatibility locus in the *Brassicaceae* genus *Leavenworthia*. *PLoS Biol* **11**(5): e1001560.
- 445   Chapman DD, Shivji MS, Louis E, Sommer J, Fletcher H, Prodöhl PA. 2007. Virgin birth in a  
446       hammerhead shark. *Biol Lett* **3**(4): 425–427.
- 447   Charlesworth D. 2002. Plant sex determination and sex chromosomes. *Heredity (Edinb)* **88**(2): 94–

- 448 101.
- 449 Charlesworth D, Charlesworth B. 1987. Inbreeding depression and its evolutionary consequences.  
450 *Annu Rev Ecol Evol Syst* **18**: 237–268.
- 451 Charlesworth D, Morgan MT, Charlesworth B. 1990. Inbreeding depression, genetic load, and the  
452 evolution of outcrossing rates in a multilocus system with no linkage. *Evolution (N Y)* **44**(6):  
453 1469.
- 454 Coelho MA, Bakkeren G, Sun S, Hood ME, Giraud T. 2017. Fungal Sex: The Basidiomycota. *Microbiol*  
455 *Spectr* **5**(3): 1–30.
- 456 Cruden RW, Lloyd RM. 1995. Embryophytes have equivalent sexual phenotypes and breeding  
457 systems: why not a common terminology to describe them? *Am J Bot* **82**(6): 816–825.
- 458 Devier B, Aguilera G, Hood ME, Giraud T. 2009. Ancient trans-specific polymorphism at pheromone  
459 receptor genes in basidiomycetes. *Genetics* **181**(1): 209–223.
- 460 Drummond AJ, Rambaut A. 2007. BEAST: Bayesian evolutionary analysis by sampling trees. *BMC Evol*  
461 *Biol* **7**(1): 1–8.
- 462 Drummond AJ, Suchard MA, Xie D, Rambaut A. 2012. Bayesian phylogenetics with BEAUti and the  
463 BEAST 1.7. *Mol Biol Evol* **29**(8): 1969–1973.
- 464 Dudgeon CL, Coulton L, Bone R, Ovenden JR, Thomas S. 2017. Switch from sexual to parthenogenetic  
465 reproduction in a zebra shark. *Sci Rep* **7**: 40537.
- 466 Ekseth OK, Kuiper M, Mironov V. 2014. OrthAgogue: an agile tool for the rapid prediction of  
467 orthology relations. *Bioinformatics* **30**(5): 734–736.
- 468 Ellinghaus D, Kurtz S, Willhoeft U. 2008. LTRharvest, an efficient and flexible software for de novo  
469 detection of LTR retrotransposons. *BMC Bioinformatics* **9**(18): 1–14.
- 470 Engelstädter J. 2017. Asexual but not clonal: evolutionary processes in automictic populations.  
471 *Genetics* **206**: 993–1009.
- 472 Faino L, Seidl MF, Datema E, van den Berg GC, Janssen A, Wittenberg AH, Thomma BP. 2015. Single-

- 473 molecule real-time sequencing combined with optical mapping yields completely finished  
474 fungal genome. *MBio* **6**(4): 1–11.
- 475 Feldheim KA, Clews A, Henningsen A, Todorov L, McDermott C, Meyers M, Bradley J, Pulver A,  
476 Anderson E, Marshall A. 2017. Multiple births by a captive swellshark *Cephaloscyllium*  
477 *ventriosum* via facultative parthenogenesis. *J Fish Biol* **90**(3): 1047–1053.
- 478 Ferreira ÁG, Amos W. 2006. Inbreeding depression and multiple regions showing heterozygote  
479 advantage in *Drosophila melanogaster* exposed to stress. *Mol Ecol* **15**(13): 3885–3893.
- 480 Fortuna TM, Namias A, Snirc A, Branca A, Hood ME, Raquin C, Shykoff JA, Giraud T. 2018. Multiple  
481 infections, relatedness and virulence in the anther-smut fungus castrating *Saponaria* plants. *Mol*  
482 *Ecol* **27**(23): 4947–4959.
- 483 Fortuna TM, Snirc A, Badouin H, Gouzy J, Siguenza S, Esquerre D, Le Prieur S, Shykoff JA, Giraud T.  
484 2016. Polymorphic microsatellite markers for the tetrapolar anther-smut fungus *Microbotryum*  
485 *saponariae* based on genome sequencing. *PLoS One* **11**(11): e0165656.
- 486 Giraud T, Yockteng R, Lo M. 2008. Mating system of the anther-smut fungus *Microbotryum*  
487 *violaceum*: selfing under heterothallism. *Eukaryot Cell* **7**(5): 765–775.
- 488 Gladieux P, Ropars J, Badouin H, Branca A, Aguilera G, de Vienne DM, Rodríguez de la Vega RC,  
489 Branco S, Giraud T. 2014. Fungal evolutionary genomics provides insight into the mechanisms of  
490 adaptive divergence in eukaryotes. *Mol Ecol* **23**(4): 753–773.
- 491 Gladieux P, Vercken E, Fontaine MC, Hood ME, Jonot O, Couloux A, Giraud T. 2011. Maintenance of  
492 fungal pathogen species that are specialized to different hosts: allopatric divergence and  
493 introgression through secondary contact. *Mol Biol Evol* **28**(1): 459–471.
- 494 Goldberg EE, Igić B. 2012. Tempo and mode in plant breeding system evolution. *Evolution (N Y)*  
495 **66**(12): 3701–3709.
- 496 Goldberg EE, Kohn JR, Lande R, Robertson KA, Smith SA, Igić B. 2010. Species selection maintains  
497 self-incompatibility. *Science (80- )* **330**(6003): 493–495.

- 498 Goudie F, Allsopp MH, Oldroyd BP. 2014. Selection on overdominant genes maintains heterozygosity  
499 along multiple chromosomes in a clonal lineage of honey bee. *Evolution (N Y)* **68**(1): 125–136.
- 500 Goudie F, Oldroyd B. 2014. Thelytoky in the honey bee. *Apidologie* **45**(3): 306–326.
- 501 Grognet P, Bidard F, Kuchly C, Ho Tong LC, Coppin E, Benkhali JA, Couloux A, Wincker P, Debuchy R,  
502 Silar P. 2014. Maintaining two mating types: structure of the mating type locus and its role in  
503 heterokaryosis in *Podospora anserina*. *Genetics* **197**(1): 421–432.
- 504 Hanschen ER, Herron MD, Wiens JJ, Nozaki H, Michod RE. 2018. Repeated evolution and reversibility  
505 of self-fertilization in the volvocine green algae. *Evolution (N Y)* **72**: 386–398.
- 506 Hereford J. 2010. Does selfing promotes local adaptation? *Am J Bot* **97**(2): 298–302.
- 507 Hood ME, Antonovics J. 2000. Intratetrad mating, heterozygosity, and the maintenance of  
508 deleterious alleles in *Microbotryum violaceum* (= *Ustilago violacea*). *Heredity (Edinb)* **85**(3):  
509 231–241.
- 510 Hood ME, Antonovics J. 2004. Mating within the meiotic tetrad and the maintenance of genomic.  
511 **166**(4): 1751–1759.
- 512 Hood ME, Katawczik M, Giraud T. 2005. Repeat-induced point mutation and the population structure  
513 of transposable elements in *Microbotryum violaceum*. *Genetics* **170**(3): 1081–1089.
- 514 Hood ME, Scott M, Hwang M. 2015. Breaking linkage between mating compatibility factors:  
515 tetrapolarity in *Microbotryum*. *Evolution (N Y)* **69**(10): 2561–2572.
- 516 Hraber P, Kuiken C, Yusim K. 2007. Evidence for human leukocyte antigen heterozygote advantage  
517 against hepatitis C virus infection. *Hepatology* **46**(6): 1713–1721.
- 518 Igic B, Lande R, Kohn JR. 2008. Loss of self-incompatibility and its evolutionary consequences source.  
519 *Int J Plant Sci Spec Issue* **169**(1): 93–104.
- 520 Jacobson DJ. 2005. Blocked recombination along the mating-type chromosomes of *Neurospora*  
521 *tetrasperma* involves both structural heterozygosity and autosomal genes. *Genetics* **171**(2):  
522 839–843.

- 523 Katoh K, Standley DM. 2013. MAFFT multiple sequence alignment software version 7: improvements  
524 in performance and usability. *Mol Biol Evol* **30**(4): 772–780.
- 525 Keeney S. 2008. Spo11 and the formatio of DNA double-strand breaks in meiosis. *Genome Dyn Stab*  
526 **2**: 81–123.
- 527 Koren S, Schatz MC, Walenz BP, Martin J, Howard JT, Ganapathy G, Wang Z, Rasko DA, McCombie  
528 RW, Jarvis ED, et al. 2012. Hybrid error correction and de novo assembly of single-molecule  
529 sequencing reads. *Nat Biotechnol* **30**(7): 693–700.
- 530 Lande R. 2015. Evolution of phenotypic plasticity in colonizing species. *Mol Ecol* **24**(9): 2038–2045.
- 531 Lande R, Schemske DW. 1985. The evolution of self-fertilization and inbreeding depression in plants.  
532 *Soc Study Evol* **39**(1): 24–40.
- 533 Lemaitre C, Braga MD V., Gautier C, Sagot MF, Tannier E, Marais GAB. 2009. Footprints of inversions  
534 at present and past pseudoautosomal boundaries in human sex chromosomes. *Genome Biol*  
535 *Evol* **1**: 56–66.
- 536 Lenormand T, Engelstädter J, Johnston SE, Wijnker E, Haag CR. 2016. Evolutionary mysteries in  
537 meiosis. *Philos Trans R Soc B* **371**: 2016001.
- 538 Lewis KR, John B. 1963. Chromosome marker. *Chromosome marker*.
- 539 Melters DP, Bradnam KR, Young HA, Telis N, May MR, Ruby JG, Sebra R, Peluso P, Eid J, Rank D, et al.  
540 2013. Comparative analysis of tandem repeats from hundreds of species reveals unique insights  
541 into centromere evolution. *Genome Biol* **14**(1): R10.
- 542 Menkis A, Jacobson DJ, Gustafsson T, Johannesson H. 2008. The mating-type chromosome in the  
543 filamentous ascomycete *Neurospora tetrasperma* represents a model for early evolution of sex  
544 chromosomes. *PLoS Genet* **4**(3): e1000030.
- 545 Mogie M. 1986. Automixis: its distribution and status. *Biol J Linn Soc* **28**(3): 321–329.
- 546 Nieuwenhuis BPS, Billiard S, Vuilleumier S, Petit E, Hood ME, Giraud T. 2013. Evolution of uni- and  
547 bifactorial sexual compatibility systems in fungi. *Heredity (Edinb)* **111**(6): 445–455.

- 548 Normark BB. 2003. The evolution of alternative genetic systems in insects. *Annu Rev Entomol* **48**(1):  
549 397–423.
- 550 Nougé O, Rode NO, Jabbour-zahab R, Ségard A, Chevin LM, Haag CR, Lenormand T. 2015. Automixis  
551 in *Artemia*: Solving a century-old controversy. *J Evol Biol* **28**(12): 2337–2348.
- 552 Ponnikas S, Sigeman H, Abbott JK, Hansson B. 2018. Why do sex chromosomes stop recombining?  
553 *Trends Genet* **34**(7): 492–503.
- 554 Raper JR. 1966. Genetics of sexuality in higher fungi. *Ronald Press New York*.
- 555 Schön I, Martens K, Van Dijk P. 2009. Apomixis: basics for non-botanists. In *Lost of Sex - The*  
556 *evolutionary biology of Parthenogenesis*, pp. 47–62, Springer, Dordrecht.
- 557 Schut E, Hemmings N, Birkhead TR. 2008. Parthenogenesis in a passerine bird, the zebra finch  
558 *Taeniopygia guttata*. *Ibis (Lond 1859)* **150**(1): 197–199.
- 559 Smit AF, Hubley RR. 2015. RepeatModeler Open-1.0. *Repeat Masker Website*.
- 560 Sonnenberg ASM, Gao W, Lavrijssen B, Hendrickx P, Sedaghat-Tellgerd N, Foulongne-Oriol M, Kong  
561 WS, Schijlen EGWM, Baars JJP, Visser RGF. 2016. A detailed analysis of the recombination  
562 landscape of the button mushroom *Agaricus bisporus* var. *bisporus*. *Fungal Genet Biol* **93**: 35–  
563 45.
- 564 Stamatakis A. 2006. RAxML-VI-HPC: Maximum likelihood-based phylogenetic analyses with  
565 thousands of taxa and mixed models. *Bioinformatics* **22**(21): 2688–2690.
- 566 Stöck M, Savary R, Betto-Colliard C, Biollay S, Jourdan-Pineau H, Perrin N. 2013. Low rates of X-Y  
567 recombination, not turnovers, account for homomorphic sex chromosomes in several diploid  
568 species of palearctic green toads (*Bufo viridis* subgroup). *J Evol Biol* **26**(3): 674–682.
- 569 Sun S, Yadav V, Billmyre RB, Cuomo CA, Nowrousian M, Wang L, Souciet JL, Boekhout T, Porcel B,  
570 Wincker P, et al. 2017a. Fungal genome and mating system transitions facilitated by  
571 chromosomal translocations involving intercentromeric recombination. *PLoS Biol* **15**(8):  
572 e2002527.

- 573 Sun Y, Svedberg J, Hiltunen M, Corcoran P, Johannesson H. 2017b. Large-scale suppression of  
574 recombination predates genomic rearrangements in *Neurospora tetrasperma*. *Nat Commun*  
575 **8**(1): 1140.
- 576 Suomalainen E. 1950. Parthenogenesis in animals. *Adv Genet* **3**: 193–253.
- 577 Termolino P, Cremona G, Consiglio MF, Conicella C. 2016. Insights into epigenetic landscape of  
578 recombination-free regions. *Chromosoma* **125**: 301–308.
- 579 Van der Beek JG, Los JA, Pijnacker LP. 1998. Cytology of parthenogenesis of five Meloidogyne species.  
580 *Fundam Appl Nematol* **21**(4): 393–399.
- 581 Van Dongen SM. 2000. Graph clustering by flow simulation  
582 (<https://dspace.library.uu.nl/handle/1874/848>).
- 583 Vekemans X, Poux C, Goubet PM, Castric V. 2014. The evolution of selfing from outcrossing ancestors  
584 in Brassicaceae: What have we learned from variation at the S-locus? *J Evol Biol* **27**(7): 1372–  
585 1385.
- 586 Vercken E, Fontaine MC, Gladieux P, Hood ME, Jonot O, Giraud T. 2010. Glacial refugia in pathogens:  
587 european genetic structure of anther-smut pathogens on *Silene latifolia* and *Silene dioica*. *PLoS*  
588 *Pathog* **6**(12): e1001229.
- 589 Walker T. 1985. Some aspects of agamospory in ferns - the Braithwaite System. *Proc R Soc Edinburgh,*  
590 *Sect B Biol Sci* **86**: 59–66.
- 591 Wang J, Na J, Yu Q, Gschwend AR, Han J, Zeng F, Aryal R, VanBuren R, Murray JE, Zhang W, et al.  
592 2012. Sequencing papaya X and Y<sup>h</sup> chromosomes reveals molecular basis of incipient sex  
593 chromosome evolution. *Proc Natl Acad Sci* **109**(34): 13710–13715.
- 594 Watts PC, Buley KR, Sanderson S, Boardman W, Ciofi C, Gibson R. 2006. Parthenogenesis in Komodo  
595 dragons. *Nature* **444**(7122): 1021.
- 596 Wright AE, Dean R, Zimmer F, Mank JE. 2016. How to make a sex chromosome. *Nat Commun* **7**:  
597 12087.

- 598 Yang Z. 2007. PAML 4: Phylogenetic analysis by maximum likelihood. *Mol Biol Evol* **24**(8): 1586–1591.
- 599 Zakharov IA. 2005. Intratetrad mating and its genetic and evolutionary consequences. *Russ J Genet*  
600 **41**(4): 402–411.
- 601 Zakharov IA. 1986. Some principles of the gene localization in eukaryotic chromosomes. Formulation  
602 of the problem and analysis of non-random localization of the mating-type loci in some fungi.  
603 *Sov Genet* **22**: 1415–1419.

## Figure legends

**Figure 1: Odds of compatibility among gametes of a diploid individual in basidiomycete fungi.** Gametes are fully compatible only if they carry different alleles at both mating-type loci, the PR (including pheromone receptor and pheromone genes, with  $a_1$  and  $a_2$  alleles) and HD (including homeodomain genes, with  $b_1$  and  $b_2$  alleles) loci. A) With PR and HD mating-type loci unlinked from each other and from the centromeres (shown here located in different chromosomes in blue and red), the percentage of compatibility of a given gamete among the other gametes produced by the same diploid individual is 25% across multiple meioses (a given gamete is compatible with one of every four gametes), and the percentage is 33% within tetrad (a given gamete is compatible with one of the other three gametes in the tetrad) or 67% (a given gamete is compatible with two of the three remaining gametes in the tetrad) depending on segregation of the mating type alleles. The different types of gametes produced are tetratypes (TT), parental ditypes (PD) or non-parental ditypes (NPD), which depends on allele segregation and on whether a crossing-over occurred between one of the two loci and the centromere. B) With PR and HD mating-type genes linked to the centromeres of different chromosomes (blue and red), the percentage of compatibility of a given gamete among the other gametes produced by the same diploid individual is 25% across multiple meioses but 67% within a tetrad (a given gamete is compatible with two of the three other gametes in the tetrad) due to the segregation of the variation occurring only at meiosis I for both mating type loci. The different types of gametes produced are parental ditypes (PD) or non-parental ditypes (NPD), which depends on segregation. C) With HD and PR loci fully linked to each other on the same chromosome, the percentage of compatibility of a given gamete among the other gametes produced by the same diploid individual is 50% across multiple meioses (a given gamete is compatible with one of every two gametes), and 67%

within a single meiotic tetrad (a given gamete is compatible with two of the three other gametes in the tetrad). The light blue background shows the opposite cells of ordered tetrads, both in a *Microbotryum* linear tetrad representation (bottom panel) and in the different types of possible tetrads depicted depending on mating-type locus linkage.

**Figure 2: Phylogenies of anther-smut fungi and their mating-type loci linkage.** A) *Microbotryomycete* phylogenetic tree based on 780 orthologous genes, including the studied *Microbotryum* species (shown in the anthers of their host plants) and the outgroup *Rhodosporidium babjevae*. The empty circles indicate full bootstrap support. Tree internode certainty with no conflict bipartitions (the normalized frequency of the most frequent bipartition across gene genealogies relative to the summed frequencies of the two most frequent bipartitions) is given above the branches, indicating good support for the bipartitions. Black bars at right indicate unlinked mating-type loci, dark grey linkage of mating-type loci to centromeres and light grey mating-type loci linkage.

**Figure 3: Intraspecific comparison of gene order between mating-type chromosomes.** Comparison of gene order between HD and PR chromosome pairs in *Microbotryum lagerheimii* (a and b) and *M. saponariae* (c and d). The outer tracks represent contigs, staggered every 200 kilobases. The HD, PR and pheromone genes are indicated by blue, dark purple and small light-purple circles, respectively. Blue and orange lines link alleles, the latter corresponding to inversions. The link width is proportional to the corresponding gene length. Yellow regions on the contig track indicate the centromeres (regions with low gene density, high TE density and enriched in tandem-repeats marked as pink marks). The black marks along the right contigs track indicate genes that have no synonymous substitutions between  $a_1$  and  $a_2$  alleles within species ( $d_s=0$ ). Green marks indicate transposable elements (TEs) and grey marks non-TE genes. The ancient regions of recombination suppression are indicated on

the outer track in blue for the HD locus and in purple for the PR locus. **a)** Comparison of the  $b_1$  (left, orange) and  $b_2$  (right, light orange) HD *M. lagerheimii* mating-type chromosomes. **b)** Comparison of the  $a_1$  (left, orange) and  $a_2$  (right, light orange) PR *M. lagerheimii* mating-type chromosomes. **c)** Comparison of the  $b_1$  (left, red) and  $b_2$  (right, light red) HD *M. saponariae* mating-type chromosomes. **d)** Comparison of the  $a_1$  (left, red) and  $a_2$  (right, light red) PR *M. saponariae* mating-type chromosomes. The large green arrow indicates the large inversion between the two mating-type chromosomes encompassing the mating-type locus and the centromere. The green regions on the contig track of each mating-type chromosome indicate the small inversion that likely occurred after the large inversion linking the PR locus to the centromere, extending the region of suppressed recombination.

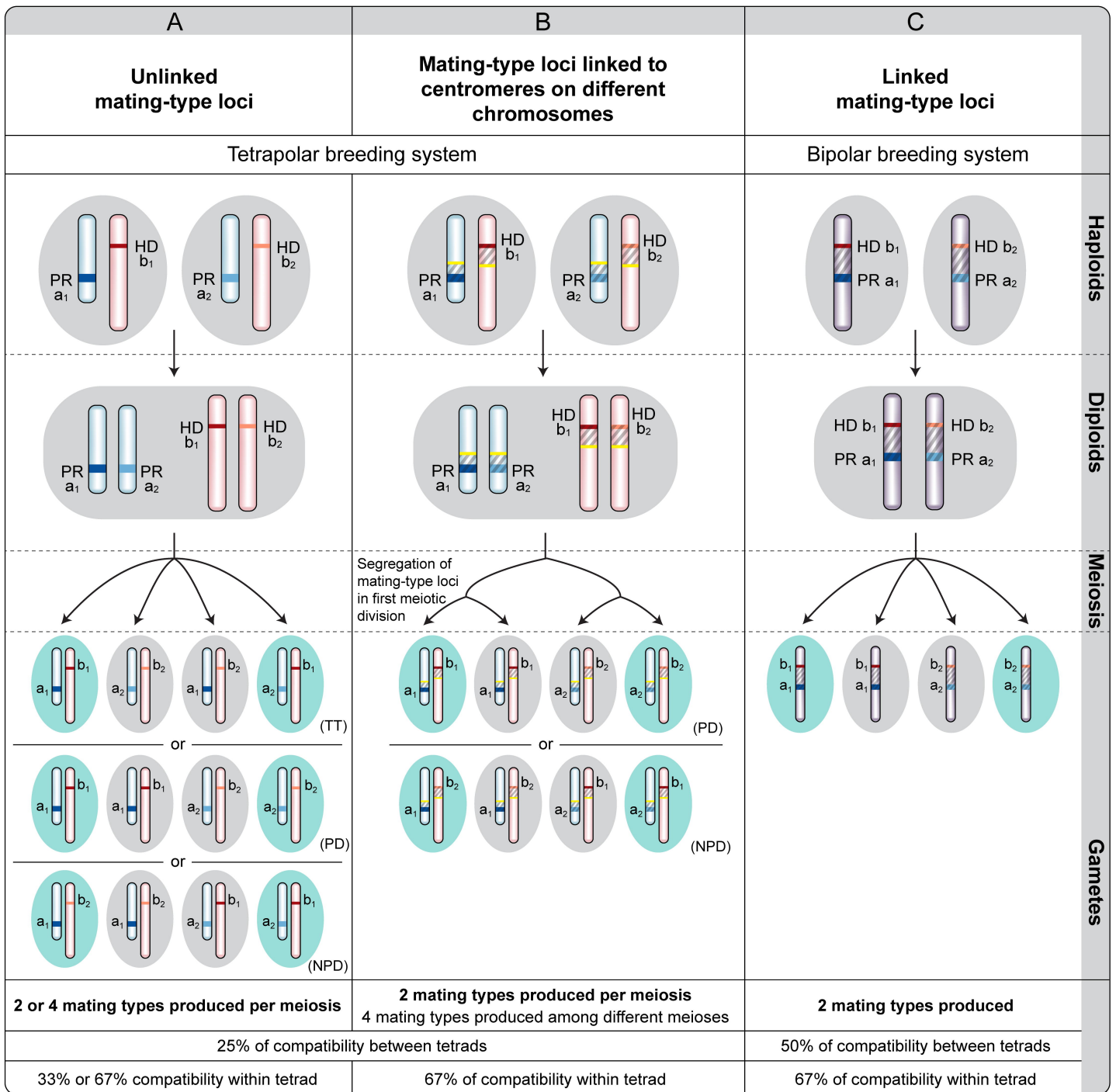
**Figure 4: Per-gene synonymous divergence and respective standard error ( $d_S \pm SE$ ) between alleles associated to the  $a_1b_1$ - $a_2b_2$  mating types along the mating-type chromosomes within diploid *Microbotryum lagerheimii* and *M. saponariae* individuals.**

Synonymous divergence is plotted against the genomic coordinates of the  $a_1 b_1$  mating-type chromosomes of *M. intermedium* for all single-copy genes shared by the mating-type chromosomes, as a proxy for ancestral gene order. Divergence between the  $a_1$  and  $a_2$  pheromone receptor (PR) was too extensive (Devier et al. 2009) and could not be computed (noted as “unalignable”). The positions of the centromeres are indicated by yellow dots. Genes with  $d_S > 0$  between mating types around the PR and HD mating-type loci in *M. lagerheimii* are colored in purple and blue, respectively. The purple and blue regions correspond to the older PR- and HD-regions of suppressed recombination that evolved before and at the base of the radiation of the clade, respectively (Branco et al. 2017, 2018). Red arrows indicate the genes used for dating recombination cessation events. **a)** Per-gene synonymous divergence between mating types in *M. lagerheimii* along the gene order of the

$a_2$  PR *M. intermedium* mating-type chromosome. **b)** Per-gene synonymous divergence between mating types in *M. lagerheimii* along the gene order of the  $b_2$  HD *M. intermedium* mating-type chromosome. **c)** Per-gene synonymous divergence between mating types in *M. saponariae* along the gene order of the  $a_2$  PR *M. intermedium* mating-type chromosome. **d)** Per-gene synonymous divergence between mating types in *M. saponariae* along the gene order of the  $b_2$  HD *M. intermedium* mating-type chromosome.

**Figure 5: Linkage date estimates across *Microbotryum*.** Linkage between mating-type loci (PR and HD) and centromeres, or between PR and HD loci was inferred from dates of divergence between alleles associated to the  $a_1$  and  $a_2$  mating types at genes linked to the mating-type loci. In gene genealogies, nodes separating alleles associated to the  $a_1$  and  $a_2$  mating types within species correspond to the date of linkage to the mating type loci (to the HD locus in blue and to the PR locus in purple). Genealogies of alleles associated to the alternative mating-types ( $a_1$  and  $a_2$ ) were reconstructed based on a concatenated alignment of both alleles at 9 genes ancestrally located between the centromere and the HD-proximal region (8,525 aligned codons) and of 10 genes ancestrally located between the centromere and the PR-proximal region (10,200 aligned codons). The genes used for this analysis, with both alleles in all species, are indicated by red arrows in the Figure 3. **a)** Marginal posterior densities for the most recent common ancestor date (MRCA time) estimated with BEAST v2.4.0 based on multiple sequence alignments of genes located between the HD-proximal (blue) or the PR-proximal (light purple) region and the corresponding centromeres in the ancestral gene order. **b)** Time-calibrated tree of  $a_1$  and  $a_2$  alleles with nodes drawn at the mean date (in million years, MY) for the genes on the HD chromosome. Inferred divergence dates for the genes located between the HD-proximal or the PR-proximal regions and the corresponding centromeres are shown in blue or purple fonts, respectively, to the right of the

nodes. Light blue and light purple bars correspond to 95% confidence intervals. Speciation dates as inferred from each dataset are shown in black font on the right side of the nodes (bottom, PR set; up, HD set).



Haploids










Diploids

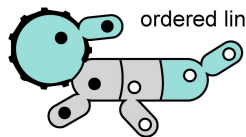
Meiosis

Gametes


Key:

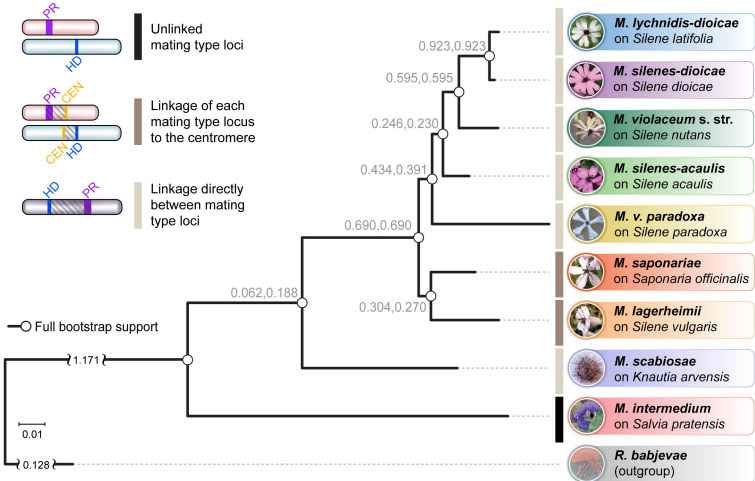
Mating-type loci

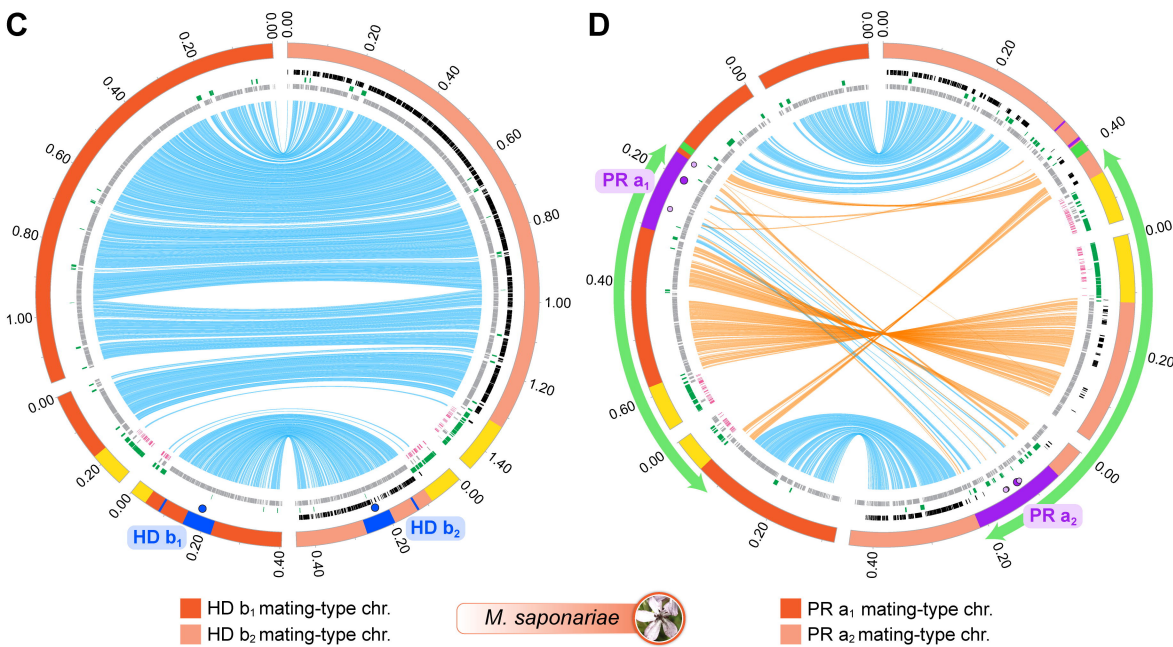
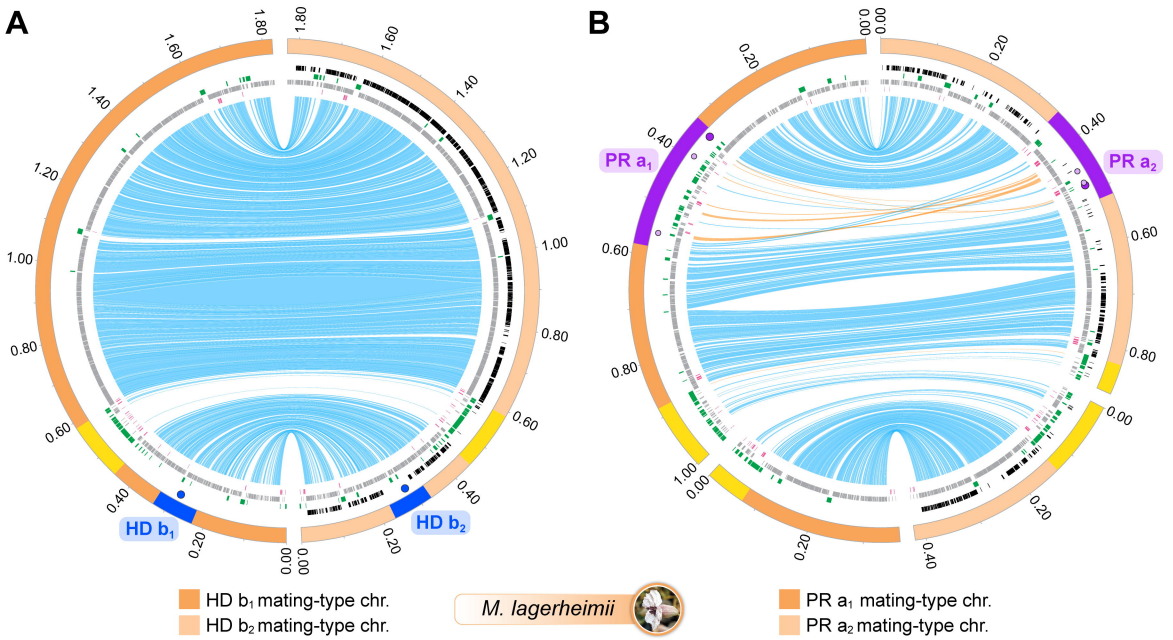
-  HD b<sub>1</sub>
-  HD b<sub>2</sub>
-  PR a<sub>1</sub>
-  PR a<sub>2</sub>
-  Fused HD/PR Chr.
-  HD Chr.
-  PR Chr.
-  centromere
-  suppression of recombination



ordered linear tetrad

 opposite cells of the linear tetrad



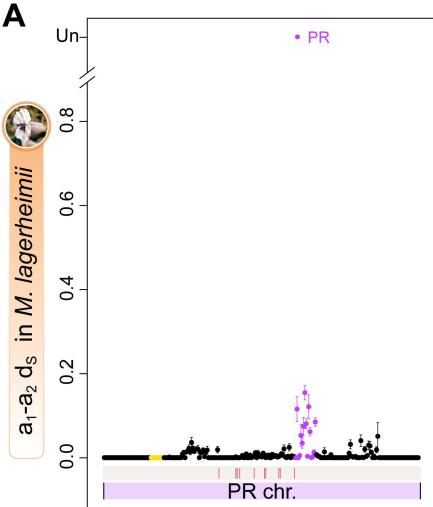


**key to tracks:**

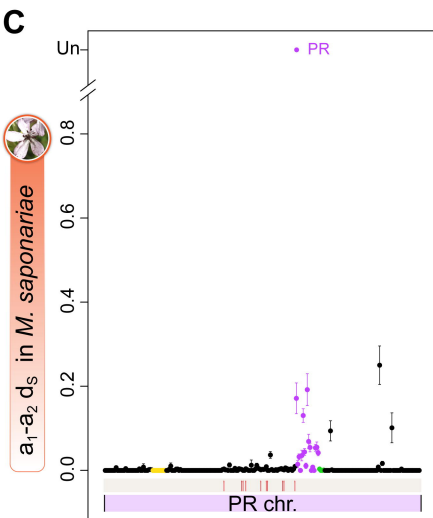
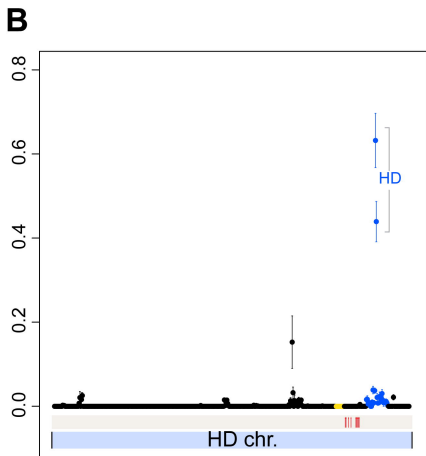
- $d_s = 0$
- Genes
- Transposable elements
- Centromeric repeats

**Links:**

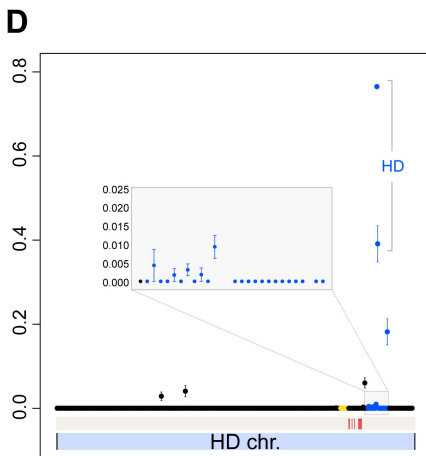
- alleles in the same orientation
- alleles in inverted orientation



Gene order along the mating-type chromosomes of *M. intermedium*



Gene order along the mating-type chromosomes of *M. intermedium*



Key: Genes used for inferences of linkage dates Centromere

